Environmental and Experimental Botany 251 (2026) 106484



Contents lists available at ScienceDirect

Environmental and Experimental Botany

journal homepage: www.elsevier.com/locate/envexpbot



Research paper

Non-enzymatic antioxidant accumulation as a potential short-term memory mechanism to drought in M2 grapevine rootstock

Sara Parri [a,*,1], Sara Anichini [b,1], Marco Romi [a], Luigi Falginella [c], Elisa De Luca [c], Giampiero Cai [a]

[a] Department of Life-Sciences, University of Siena, Via Mattioli 4, Siena 53100, Italy
[b] Department of Agriculture, Food, Environment and Forestry (DAGRI), University of Florence, Piazzale delle Cascine 18, Florence 50144, Italy
[c] VCR Research Center, Via Ruggero Forti 4, San Giorgio della Richinvelda, 33095, Italy

ARTICLE INFO

Keywords:
Vitis spp.
Gas exchange
Soluble sugars
Antioxidants
Polyphenols
Phenylpropanoids

ABSTRACT

Recurrent drought events, exacerbated by climate change, pose a growing threat to grapevine productivity and wine quality worldwide. While long-term structural and epigenetic stress memory in grapevine is well documented, the biochemical mechanisms underlying short-term, within-season memory remain poorly understood. This study investigated short-term drought stress memory in the M2 rootstock genotype under controlled growth chamber conditions. Plants were subjected to four treatments - well-watered, early-short drought, late-long drought, and double drought - across two stress periods separated by a full recovery phase. Gas exchange, relative water content, electrolyte leakage, soluble sugars, total polyphenols, flavonoids, and key stress-responsive proteins were monitored throughout the experiment. Results indicate that prior drought exposure conferred no advantage in stomatal regulation or water status management. However, double drought significantly enhanced membrane integrity compared to late-long drought alone, as shown by lower electrolyte leakage, alongside a markedly higher accumulation of total polyphenols and flavonoids. This non-enzymatic antioxidant response was underpinned by accumulation of the enzymes 5-enolpyruvylshikimate-3-phosphate synthase and chalcone synthase during the early-short stress and recovery, suggesting that the shikimate and phenylpropanoid pathways may serve as the molecular imprint of short-term drought stress memory in grapevine.

1. Introduction

In the context of ongoing climate change, the grapevine (*Vitis vinifera* L.) is increasingly exposed to recurrent abiotic stresses, such as drought, heatwaves and flooding. These environmental pressures directly impact vine physiology, resulting in reduced berry quality and posing a threat to the long-term sustainability of viticulture in key wine-producing regions (Botton et al., 2022; Canton et al., 2025). Although grapevine is generally considered drought-tolerant due to its deep root system and versatile stomatal regulation, its productivity drops dramatically under suboptimal water availability (Chaves et al., 2010; Lovisolo et al., 2010). This highlights the need for a better understanding of the mechanisms underlying grapevine resilience and adaptive capacity in the context of fluctuating water availability.

To cope with environmental constraints, plants have evolved mechanisms that enable them to retain information about previous stress events. This process is known as 'stress memory' or 'priming' (Sun et al., 2024; Zamorano et al., 2021). Following initial exposure to stress, plants enter a primed physiological state that enhances their response to subsequent stress events (Nagahatenna et al., 2022; Zamorano et al., 2021). Stress memory can occur at different levels, including within the lifespan of the individual plant, transmission to vegetative or sexual progeny, and, in some cases, persistence across multiple generations (Lämke and Bäurle, 2017; Nagahatenna et al., 2022). While initial stress can impair plant performance, the development of stress memory is an adaptive strategy that enhances long-term resilience and survival in challenging environments by optimising the primed plant's response to recurring stress (Nagahatenna et al., 2022; Venios et al., 2024; Zamorano et al., 2021).

The study of stress memory in grapevines has primarily focused on

* Corresponding author.
E-mail address: sara.parri2@unisi.it (S. Parri).
[1] These authors contributed equally to this work.

https://doi.org/10.1016/j.envexpbot.2026.106484
Received 31 July 2026; Received in revised form 22 October 2026; Accepted 24 October 2026
Available online 26 October 2026
0098-8472/© 2026 The Authors. Published by Elsevier B.V. This is an open access article under the CC BY license (http://creativecommons.org/licenses/by/4.0/).

long-term or multi-seasonal drought exposure. The most well-documented forms of this phenomenon are anatomical and epigenetic adjustments. Epigenetic regulation, such as DNA methylation and post-translational histone modifications (e.g. H3K27me3 or H3K4me3), can modulate gene expression without altering the DNA sequence. This contributes to the development of long-lasting somatic memory (Pereira et al., 2025; Venios et al., 2024; Zhu et al., 2023). In perennial crops such as grapevines, these changes can be maintained during recovery and propagated through mitotic divisions, thereby supporting stress imprinting across growing seasons (Pereira et al., 2025; Venios et al., 2024). In addition to epigenetic mechanisms, recurrent drought can induce structural adjustments that persist over time. For instance, limited water availability during the early stages of cambial growth can result in the formation of narrower xylem vessels. This leads to reduced transpiration rates and increased hydraulic conductivity plasticity, ultimately enhancing water use efficiency. This 'structural memory' has been shown to persist across developmental stages and even between seasons (Munitz et al., 2018; Netzer et al., 2019; Tombesi et al., 2018; Zamorano et al., 2021). Other molecular processes have been suggested to support transcriptional adaptation to oxidative stress. Examples include alternative splicing memory induced by priming with hydrogen peroxide (Sun et al., 2024; Zuo et al., 2024). Taken together, these findings suggest that grapevines can integrate and store stress-related information across multiple biological levels, particularly when exposed to repeated or long-term stress.

Unlike long-term memory, the study of short-term stress memory in grapevines has received comparatively little attention, despite its potential relevance to plant performance and berry quality within a single growing season (Canton et al., 2025; Merli et al., 2016). This form of memory is primarily associated with temporary biochemical and physiological changes that persist after the stressor has been removed or are rapidly reactivated upon subsequent exposure. The accumulation of gamma-aminobutyric acid (GABA) is among the proposed indicators of short-term memory and has been shown to improve gas exchange and stress tolerance during recurrent drought events (Nagahatenna et al., 2022). Similarly, repeated stressful events can alter the dynamics of non-structural carbohydrates, with an increase in soluble sugars contributing to osmotic adjustment and cellular protection (Canton et al., 2025; Peng et al., 2023). Stomatal closure is one of the first physiological responses to drought. This process is both rapid and reversible, and the subsequent reduction in photosynthesis could be a preparatory strategy for the next drought (Sadhukhan et al., 2022). However, stomatal closure inevitably leads to photo-oxidative stress and the rapid accumulation of reactive oxygen species (ROS), which cause oxidative damage to proteins, lipids and nucleic acids if their accumulation is not efficiently controlled (Dinis et al., 2018; Peng et al., 2023). The antioxidant system therefore plays a pivotal role in both the immediate stress response and stress memory formation. Enzymatic antioxidants, such as superoxide dismutase (SOD), catalase (CAT) and ascorbate peroxidase (Dinis et al., 2018; Peng et al., 2023), and non-enzymatic compounds, particularly polyphenols such as flavonoids and phenolic acids (Król and Weidner, 2017), work to remove ROS and reduce oxidative damage during and after stressful events. These phenolic compounds are largely synthesised through the shikimate and phenylpropanoid pathways, with phenylalanine ammonia-lyase (PAL) and chalcone synthase (CHS) acting as key regulatory enzymes that connect primary metabolism to the production of flavonoids, condensed tannins and other polyphenols (Winkel-Shirley, 2002). Together, these biochemical responses may represent short-term informational imprints that influence plant performance in the event of repeated drought.

In grafted grapevines, the rootstock plays a key role in modulating stress responses by acting as the primary sensor of soil water deficit. When drought conditions are perceived, the root system initiates a complex, long-distance signaling cascade involving hydraulic signals and phytohormones that travels upwards to the scion. Consequently, while the stress is initially detected below ground, its physiological and biochemical effects are observed in the leaves. Accordingly, the degree of drought tolerance expressed by the canopy depends markedly on the specific rootstock/scion combination, which determines the intensity of the hydraulic and biochemical signals reaching the leaves (Daler et al., 2024a). Investigating foliar responses, such as changes in primary and secondary metabolites, provides crucial insights into how rootstock-driven signals are translated into systemic physiological acclimation and long-term stress tolerance. This study examines how the M2 grapevine genotype responds to short-term drought stress memory in a controlled growth chamber environment. The M2 genotypes belong to the recently released M-series of grapevine rootstocks, which are not well characterised. In addition, a previous study revealed that it exhibited several significant responses to water-deficiency stress, including high levels of suberisation in the Caspary strip (Anichini et al., 2026a). These observations prompted us to investigate the drought stress response in M2 further. It focuses on the shoot's intrinsic physiological and metabolic responses to water priming, independent of grafting. We assess whether repeated stress exposure induces measurable biochemical imprints that modulate physiological performance during subsequent stress by applying two consecutive short drought events separated by a full recovery period. These imprints include changes in soluble sugars, polyphenols, antioxidant capacity, and stress-related proteins. We hypothesise that: (i) plants exposed to repeated drought events will exhibit enhanced tolerance compared to non-primed plants; (ii) this primed state is associated with specific biochemical adjustments that persist after recovery or are reactivated more rapidly upon re-stress; (iii) given the central role of the antioxidant system, primed plants will exhibit pre-accumulation or rapid re-induction of antioxidant secondary metabolites, as well as of the shikimate and phenylpropanoid pathways. This enables a more effective response to subsequent stress events.

2. Materials and methods

2.1. Plant material and growth conditions

The experiment was carried out on M2 vine rootstock (cv. Cosmo 10 x cv. 140 Ruggeri) provided by Vivai Cooperativi Rauscedo (VCR), (Rauscedo, PN, Italy). The cuttings were initially rehydrated for 24 h before being rooted by immersing the basal node in a 0.3% (3000 ppm) solution of indole-3-butyric acid (IBA; Merck, Rahway, NJ, USA) and then grown in an aeroponic system at the Santa Chiara Lab, University of Siena for one year. Finally, they were transferred to a controlled environment located in the same building (Microcosmo, FOS S.p.A., Genoa, Italy and ENEA, Rome, Italy; https://pianogreen.com/microcosmo/). The substrate used consisted primarily of sand and clay soil collected from a Chianti Classico farm (Brolio, Località Madonna a Brolio, 53013 Gaiole in Chianti (SI), Italy, 43.413341° N, 11.463499° E). A surface layer of universal potting soil was applied to facilitate planting. Inside the Microcosmo, the following environmental parameters were maintained: a photoperiod of 16/8 with a red:blue light ratio of 3:1 plus white light, providing a total incident radiation of 200 μmol m^{-2} s^{-1} at the canopy level. The temperature remained at 27 °C between 7 a.m. and 10 p.m., dropping to 23 °C for the remaining hours. Relative humidity was set at 60%.

2.2. Repeated drought stress treatment

Following a 30-day acclimation period, plants were subjected to a repeated drought stress period to investigate memory effects. The 4 treatment groups were: (1) ww-ww (well-watered - well-watered), namely control plants maintained under constant irrigation; (2) ww-ds (well-watered - drought-stressed), plants subjected only to the late-longdrought stress; (3) ds-ww (drought-stressed - well-watered), plants subjected only to the early-short drought stress, followed by a recovery period; (4) ds-ds (drought-stressed - drought-stressed), plants subjected

to both the first and second drought stresses. Each experimental group consists of 6 individuals. The experimental timeline is shown in Fig. 1.

Soil moisture was continuously monitored using three probes per treatment (TDSPSM02.015, Ageon, Cuneo, Italy). The well-watered groups were maintained at a soil moisture content above 60% (v:v). Drought stress was defined as a sustained drop in soil moisture to 30% (v:v).

Gas exchange parameters were repeatedly recorded during the experimental period: on the last day ("d") of the acclimation period (d01); during the first stress period (t1) on d6, d8 and d10; during the recovery period (t2) on d14, d21 and d23; and during the second drought stress period (t3) on days d27, d32, d35, d38 and d41.

For end-point analyses, experimental groups were pooled based on the current irrigation status during the initial stages to minimize the reduction in canopy size and avoid influencing subsequent, non-destructive gas exchange measurements. The sampling groups were defined as follows: for t0, a single pooled group was defined as 'well-watered' (ww), which included all future ww, ww-ds, ds-ww and ds-ds plants; for t1 and t2, two pooled groups were defined: 'well-watered' (ww) (comprising future ww and ww-ds plants) and 'drought-stressed' (ds) (comprising future ds and ds-ww plants); for t3, all four final groups were sampled individually (ww-ww, ww-ds, ds-ww and ds-ds). Relative water content and electrolyte leakage were measured around 9:00 a.m. on the final day of each experimental period (t0, t1, t2, t3). Subsequently, at 2:00 p.m. on the same days, 7 full expanded, mature leaves from each experimental group were sampled, immediately frozen in liquid nitrogen, and stored at −80°C for subsequent analyses.

2.3. Gas exchange analysis and chlorophyll fluorescence

The parameters of net carbon assimilation (A), stomatal conductance (g_{sw}) and photosystem II actual efficiency (ΦPSII) were measured on 5 fully expanded mature leaves at all the previously defined days for each time-point. Data were acquired with a portable LI-6800 gas exchange analyzer (LI-COR Biosciences, Lincoln, NE, USA), which was equipped with an integrated chlorophyll fluorescence chamber. During the measurements, the following environmental settings were established: a chamber area of 2 cm^2, CO_2 concentration fixed at 400 ppm, relative humidity set to 60%, block temperature maintained at 25°C, and photosynthetic active radiation (PAR) at 2000 µmol m^{-2} s^{-1} (Kar et al., 2021; Villalobos-Soublett et al., 2022). The maximum quantum yield of PSII (F_v/F_m), i.e. the maximum efficiency with which PSII converts absorbed light energy into photochemistry when all reaction centers are open, was also measured after dark adaptation (leaves were covered with aluminum foil for at least 20 min (Hajizadeh Sisakhti et al., 2025)).

2.4. Relative Water Content

The Relative Water Content (RWC) of the leaves was calculated as described by El Yamani et al. (2019). Six fully expanded and mature leaves for groups at each time point were cut below the petiole, immediately placed in pre-weighed tubes, and weighed to obtain the fresh weight (FW). The tubes were then filled with distilled water and the samples incubated for 24 h at 4°C in the dark. The leaves were then removed from the tubes and dried with paper towels to absorb excess water. The samples were weighed to determine the turgid weight (TW). Finally, the samples were placed in paper bags and heated in an oven at 80 °C for 48 h, after which they were weighed to determine their dry weight (DW). The leaf RWC was calculated as:

$$RWC \quad (\%) \quad = \quad \frac{(FW \quad - \quad DW)}{(TW \quad - \quad DW)}$$

2.5. Electrolyte leakage

The cell membrane permeability to solutes was assessed by measuring the electrolyte leakage (EL) according to Parri et al. (2023). Two leaf discs with a 0.5 cm diameter were cut from a fresh leaf and placed inside capped tubes filled with 10 mL deionised water. The samples (n = 6) were incubated for 3 h at 37°C. Following incubation, the electrical conductivity (E1) of the solution was measured using the conductivity probe of an Äkta Pure system (Cytiva, Marlborough, MA, USA). Then, the samples were heated at 95°C for 30 min before measuring the conductivity again (E2). The EL was calculated as:

EL = (E1/E2) x 100

2.6. Antioxidants content

The extraction of antioxidants was carried out on leaf tissue using 70% acetone. Briefly, the frozen leaves were weighed. After adding 70%

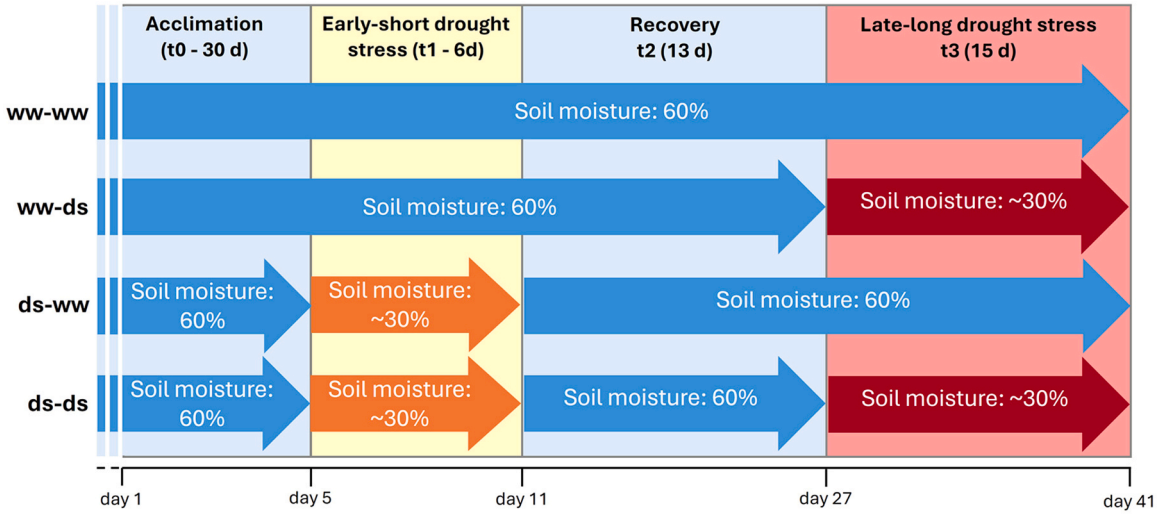


Fig. 1. Experimental design and soil moisture conditions applied during the study. Plants were subjected to four treatments (ww-ww, ww-ds, ds-ww and ds-ds) across four phases: acclimation (t0, 30 days), early-short drought stress (t1, 6 days), recovery period (t2, 13 days) and late-long drought stress (t3, 15 days). Well-watered conditions (ww) were maintained at 60% soil moisture, while drought stress conditions (ds) were imposed at about 30% soil moisture during t1 and t3. Arrows indicate the progression of treatments over time for each condition.

acetone at a ratio of 1:6 (w/v), the samples were pulverised in a Mixer Mill MM 400 (Retsch GmbH, Haan, Germany) for 8 min at 30 Hz, after which they were sonicated for 15 min. After centrifugation at 13,000*g* for 5 min, the supernatant was used for the subsequent colorimetric assays. All analyses were performed in biological triplicate.

The total polyphenol content was determined using the Folin-Ciocalteu method (Singleton and Rossi, 1965). The reaction mixture was prepared by adding 1 μL of the extract (distilled water for the blank), 230 μL of distilled water, 12.5 μL of Folin-Ciocâlteu reagent and 37.5 μL of a saturated sodium carbonate solution. The mixture was then incubated at 37 °C for 30 min and the absorbance measured at 795 nm using a microplate reader. Total polyphenolic content was calculated using a gallic acid standard curve and expressed as milligrams of gallic acid equivalents (GAE) per 100 g of fresh leaf. Total flavonoid content was determined using the aluminium chloride method (Smirnova and Pervykh, 1998). The reaction mixture was prepared by adding 12.5 μL of extract (distilled water for the blank), 75 μL of 95% ethanol, 5 μL of 10% aluminium chloride, 5 μL of 9.8% potassium acetate and 152.5 μL of distilled water. The mixtures were then incubated at room temperature for 1 h and the absorbance was measured at 415 nm using a microplate reader. Total flavonoid concentration was calculated from a quercetin standard curve and expressed as milligrams of quercetin equivalents (QE) per 100 g of fresh leaf.

2.7. Sugar content

To determine dry weight, 0.2 g of frozen leaf powder was dried at 70°C for 24 h, as described by Parri et al. (2024). Soluble sugar extraction was carried out using 1 mL of distilled water. The tissue was homogenised using a Mixer Mill MM 400 (Retsch GmbH, Haan, Germany) for 4 min at 30 Hz, then incubated at 60 °C for 10 min and treated with ultrasound for 7 min. After centrifugation (16,000 ×g for 5 min), the resulting supernatant was collected and the pellet was subjected to a second extraction. The combined supernatants were filtered (0.45 μm). High-performance liquid chromatography was performed by ISVEA (https://www.isvea.it/, Poggibonsi, Siena, Italy) using a Rezex™ RFQ-Fast Acid H^+ (8%) column (100 × 7.8 mm; Phenomenex, Torrance, CA, USA), according to the OIV-MA-AS311–03 protocol (https://www.oiv.it/). The results are expressed as the mean ± standard deviation of three biological replicates in mg/g DW.

2.8. Electrophoresis and Western blot analysis

Proteins were extracted according to Anichini et al. (2026b) starting with a pooled leaf powder made from leaves sampled from three different plants. Protein samples were separated using Bio-Rad Stain-Free SDS-PAGE gels (12%) in a Mini-PROTEAN Tetra Cell (Bio-Rad Laboratories, Inc., Hercules, CA, USA). Gels were run in Tris/Glycine/SDS running buffer (25 mM Tris, 192 mM Glycine, 0.1% SDS, pH ~8.3) at 200 V for approximately 45 min. After electrophoresis, stain-free imaging was performed using a Bio-Rad ChemiDoc Imaging System to verify protein separation and loading. Proteins were transferred to nitrocellulose membranes using the Bio-Rad Trans-Blot Turbo Transfer System following the manufacturer's protocol (typically 25 V, 1.3 A for 7 min). Membranes were blocked with EveryBlot Blocking Buffer for 5 min at room temperature with gentle agitation and then incubated for 1 h at room temperature with gentle rocking with the following primary antibodies: anti-dehydrin (1:1000, AS07206A Agrisera); anti-osmotin (1:1000, AS194336 Agrisera); anti-HSP70 (1:5000, AS08371 Agrisera); anti-CAT (1:1000, AS09501 Agrisera); anti-Cu/ZnSOD (1:1500, AS184243 Agrisera); anti-PAL 1–4 (1:1000, AS214614 Agrisera); anti-CHS (1:3000, AS122615 Agrisera); anti-EPSP synthase (1:1000, AS142782 Agrisera). After incubation, membranes were washed 2 times for 5 min each in TBS-T buffer (20 mM Tris, 150 mM NaCl, 0.1% Tween-20, pH 7.4). Secondary antibody anti-rabbit IgG conjugated with StarBright 700 fluorophores (12004161 Bio-Rad Laboratories) were diluted 1:2500 in EveryBlot Blocking Buffer and incubated for 1 h at room temperature. Membranes were then washed 2 times for 5 min each in the TBS-T buffer. Detection was performed using the Bio-Rad ChemiDoc Imaging System under fluorescence settings appropriate for StarBright 700. Target protein intensities were quantified using Bio-Rad Image Lab software and normalized via a total protein normalization. Following automated lane detection and manual boundary refinement, lane-specific normalization factors were derived from the integrated Stain-Free signal relative to a control reference lane.

2.9. Statistical analysis

To assess the overall effects of the two stress events over the experiment, g_{sw}, A, ΦPSII and F_v/F_m data were analysed by three-way ANOVA with early-short stress, late-long stress and timepoint as factors. Each measurement was treated as an independent observation. Type III sums of squares were used to account for the different number of measurement days per timepoint, and F-tests were computed with heteroscedasticity-consistent (HC3) standard errors (car package in R). P-values are reported in Table 1. For g_{sw}, A, ΦPSII and F_v/F_m, a separate one-way ANOVA was performed for each measurement day to test the effect of the irrigation treatment. Normality of residuals and homogeneity of variances were checked with the Shapiro-Wilk and Levene tests, respectively. When both assumptions were met, ANOVA was followed by Tukey's HSD test. Otherwise, data were log-transformed and the assumptions re-tested. If they were then met, ANOVA and Tukey's test were applied to the log-transformed data. If variances remained heterogeneous, Welch's ANOVA followed by the Games-Howell test was used. If residuals remained non-normal, the Kruskal-Wallis test followed by Dunn's test with Holm correction was applied. RWC, EL, glucose, fructose, total polyphenol and flavonoid contents were analysed by one-way ANOVA to test the effect of the irrigation treatment, after normality and homoscedasticity had been verified with the Shapiro-Wilk and Levene tests. Biological replicates (individual plants or independent pooled samples) were used as the experimental unit. For all analyses, post hoc tests were performed only when the overall test was significant ($p < 0.05$), and significant differences between groups are indicated in the figures by different letters. Statistical analyses and graphs were performed in R studio (2023.06.0 Build 421© 2009–2023 Posit Software, PBC) using the package ggplot2.

3. Results

The three-way ANOVA (Table 1) showed that both early-short stress and the late-long one affected g_{sw}, A and ΦPSII in a timepoint-dependent manner, as indicated by the significant early-short stress × Timepoint and late-long stress × Timepoint interactions. F_v/F_m was not affected by the treatments. The early-short stress × late-long stress × timepoint interaction, which would indicate that the response to the second stress depended on previous exposure to the first, was not significant for any

Table 1
The statistical significance of the factors early-short stress (ESS), late-long stress (LLS), timepoint (T) and their interaction on the parameters stomatal conductance (g_{sw}), net carbon assimilation (A), actual efficiency of the photosystem II (ΦPSII), and maximum efficiency of the photosystem II (F_v/F_m) calculated by the three-way ANOVA.

Parameter: *p - value*:	g_{sw}	A	ΦPSII	F_v/F_m
Early-short stress (ESS)	< 0.001	< 0.001	0.008	0.795
Late-long stress (LLS)	0.671	0.452	0.970	0.806
ESS × LLS	0.011	0.265	0.365	0.309
Timepoint (T)	< 0.001	< 0.001	< 0.001	0.384
ESS × T	< 0.001	< 0.001	0.038	0.416
LLS × T	< 0.001	< 0.001	< 0.001	0.246
ESS × LLS × T	0.083	0.089	0.504	0.721

physiological parameter.

Fig. 2 shows the gas exchange parameters monitored on different days throughout the experimental phases. Stomatal conductance (Fig. 2A) was highly sensitive to drought conditions. During the early-short drought stress period (t1), both stressed groups (ds-ds and ds-ww) exhibited a comparable reduction. This was significantly different to that observed in the well-watered groups (ww-ds and ww-ww) from day 8 until the recovery period. There were no statistical differences between the ww and ds groups during the recovery period until the first monitoring day of t3 (d27). Applying a late-long drought stress resulted in a linear decrease in g_{sw} in both the ds-ds and ww-ds groups. Following the g_{sw} trend, net carbon assimilation (Fig. 2B) accurately reflected the current irrigation status of the experimental groups, revealing statistically significant differences between the drought-stressed and control groups at t1 and t3. There were no differences related to previous stress exposure, e.g. between the ds-ds and ww-ds groups. Similarly, ΦPSII (Fig. 2C) differed significantly between the well-watered and drought-stressed groups. However, no significant differences were detected between the ds-ww and ds-ds groups during the early-short drought stress period, or between the ww-ds and ds-ds groups during the late-long one. Finally, F_v/F_m (Fig. 2D) shows no differences throughout the entire experimental period.

The relative water content of the leaves (Fig. 3A) corresponded to the irrigation levels applied to the experimental groups. It was 92% in the well-watered samples, decreasing to 87% in the drought-stressed group during the initial stress period. After full recovery, it fell to around 80% by the end of the late-long drought stress period. Although the RWC of ds-ds was slightly higher than that of ww-ds during this period, no statistically significant differences were observed. The content of glucose (Fig. 3B) and fructose (Fig. 3C) both increased in the stressed group during the early-short drought period. After full recovery, these levels were comparable to those of the control group. Interestingly, at t3, glucose and fructose accumulated mainly in the ds-ds group, whereas in all the other groups they remained similar to the control group (ww-ww), regardless of current irrigation status.

Electrolyte leakage (Fig. 4A) was measured only at t0 and t3. At t0 ww group exhibited a membrane permeability to ions around 12%. By the end of the late-long drought stress period, the recovered ds-ww group exhibited values similar to those of the controls. Interestingly, the ds-ds group showed an EL equivalent to that of the ww-ww group. In contrast, the ww-ds group had a higher and significantly different value from all the other groups.

Analysis of total polyphenol content (Fig. 4B) revealed a consistent level at t0, t1 and t2: no significant differences were observed between the ww and ds groups during the early-short drought period and subsequent recovery phase. Notably, the highest value was reached by the ds-ds group during the late-long drought period, when it differed significantly from all the other groups. Conversely, the ww-ds group exhibited a polyphenol content similar to the ww-ww group, while the lowest content was observed in the ds-ww group. The trend in flavonoid content (Fig. 4C) was similar to that in TPC. Only the ds-ds group subjected to double drought periods showed an increase in flavonoids, with results that were significantly different to those of the ww-ww, ds-ww and ww-ds groups.

The biochemical status of grapevine leaves was also evaluated by monitoring the accumulation of various proteins potentially involved in the stress response. In the case of dehydrins, the immunoreactive profile was characterised by the presence of multiple bands at 150, 65, 41, 39 and 31 kDa (Fig. 5). During the early-short drought and subsequent recovery, the dominant band was the 150 kDa band (Fig. 6A). Overall, the samples subjected to drought stress showed an increase in DEHs at both t1 and t2 compared to the control. Under late-long drought at t3, the signals of the different molecular weight bands were more similar, with a reduced relative accumulation of the 150 kDa band. Unlike the early-short stress response, after the late-long drought, stressed samples exhibited lower accumulation than the well-watered samples. Within

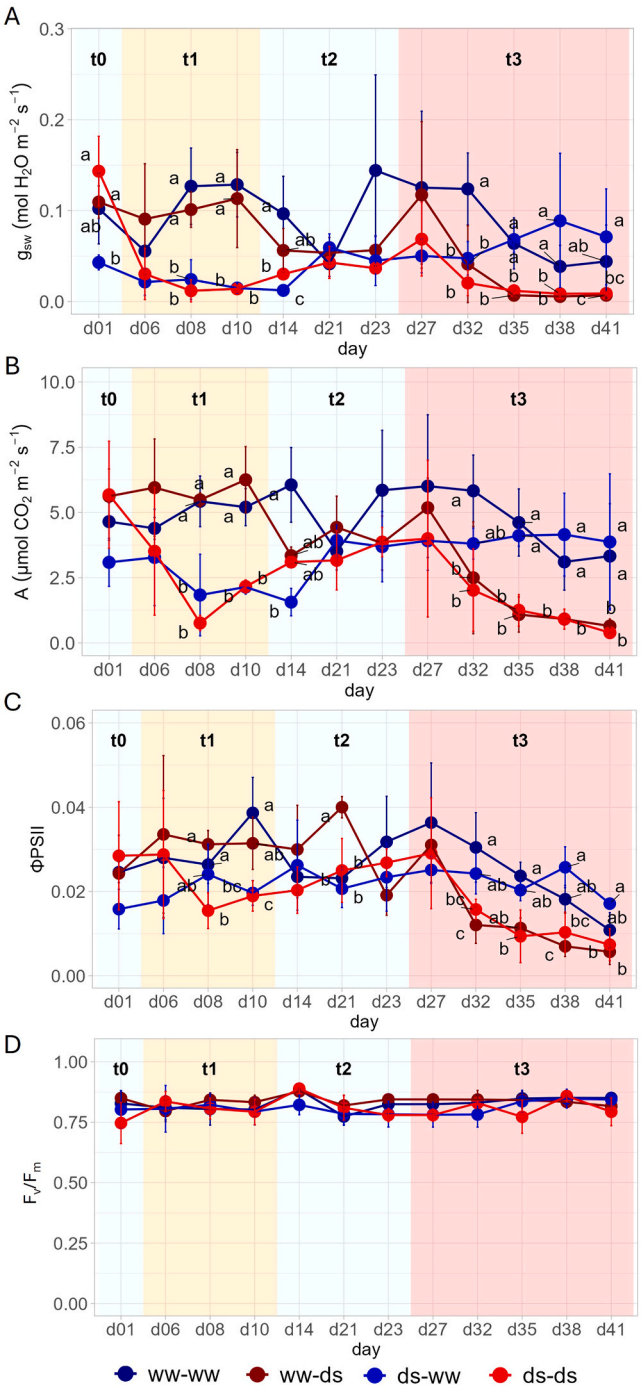


Fig. 2. Temporal dynamics of gas exchange parameters under different water treatments. (A) Stomatal conductance (g_{sw}, mol H_2O m^{-2} s^{-1}); (B) net photosynthetic rate (A, µmol CO_2 m^{-2} s^{-1}); (C) photosystem II actual efficiency (ΦPSII) and (D) maximum quantum yield of photosystem II (F_v/F_m) measured over time (days). Data are shown for different treatments (the combinations phases of well watered, ww and drought stressed, ds, groups) across four phases: acclimation (t_0), first drought stress (t_1), recovery (t_2), and second drought stress (t_3), indicated by background shading. Points represent mean values with error bars indicating standard deviation. Different letters indicate significant differences ($p < 0.05$) among treatments within each sampling day according to the post hoc tests.

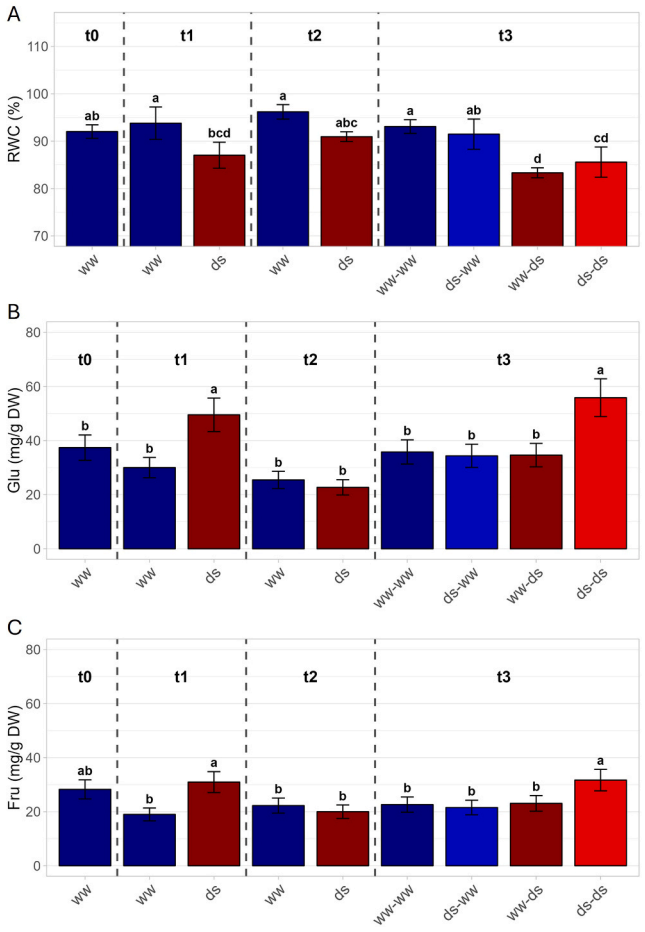


Fig. 3. Effects of water treatments on physiological and biochemical traits across experimental phases. (A) Relative water content (%), (B) glucose concentration (mg g^{-1} DW), and (C) fructose concentration (mg g^{-1} DW) measured at the end of each experimental treatment: acclimation (t_0), first drought stress (t_1), recovery (t_2), and second drought stress (t_3), separated by dashed vertical lines. Bars represent different treatments (well watered, ww and drought stressed, ds, and their combinations across phases), with mean values and error bars indicating standard deviation. Different letters indicate significant differences ($p < 0.05$) among treatments according to Tukey post hoc test.

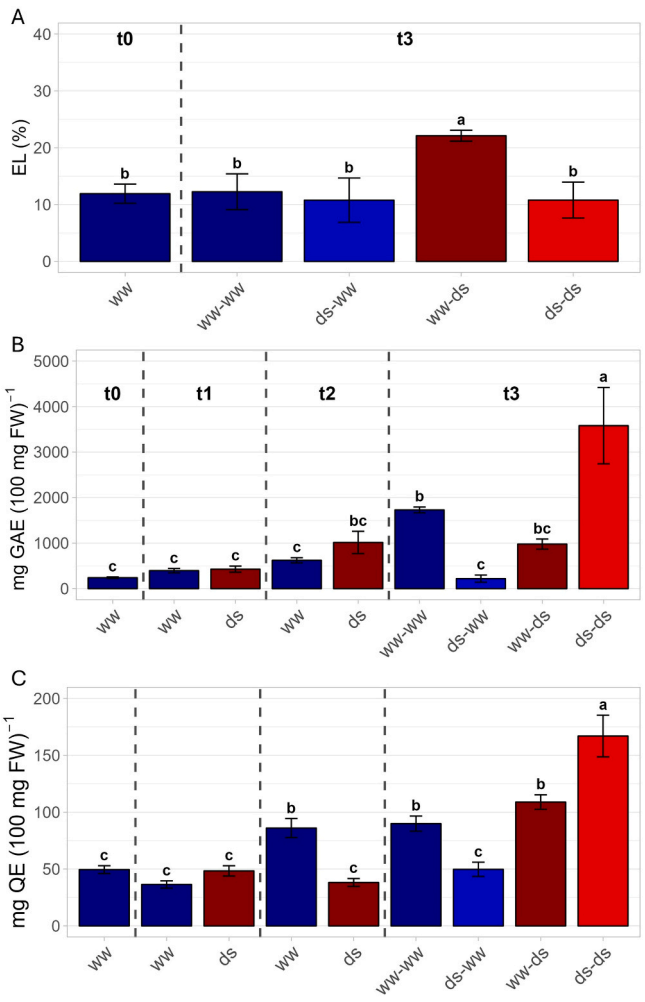


Fig. 4. Biochemical responses under different water treatments across experimental phases. (A) Electrolyte leakage (EL, %) measured at acclimation (t_0) and second drought stress (t_3). (B) Total polyphenol content (mg gallic acid/100 mg FW)and (C) flavonoid content (mg quercetin equivalent/100 mg FW)measured during acclimation (t_0), first drought stress (t_1), recovery (t_2), and second drought stress (t_3), separated by dashed vertical lines. Bars represent different treatments (well watered, ww and drought stressed, ds, and their combinations across phases), with mean values and error bars indicating standard deviation. Different letters indicate significant differences ($p < 0.05$) among treatments according to Tukey post hoc test.

the drought-stressed samples, the ds-ds group showed lower values than the ww-ds group.

Osmotin was represented by a 25 kDa band (see Fig. 5). Quantification revealed that OSM levels were higher in ds than in ww at both t1 and t2 (Fig. 6B). However, a higher accumulation was observed during recovery than the early-short stress compared to the control. At t3, the peak signal was observed in ww-ww, while a reduction was seen in the other conditions. Specifically, the ww-ds, ds-ww and ds-ds conditions all exhibited lower values than the control condition, with relatively minor variations between them.

Catalase is represented by a 51 kDa band (Fig. 5). Fig. 6C shows that, at t1, CAT accumulation in the ds group was only slightly higher than in the ww group. This difference increased during recovery at t2. At t3 the highest value was observed in the ww-ww group; under the other conditions, a clear reduction in the signal was evident. Of the stressed groups, the accumulation of CAT in ww-ds was twice that in ds-ds.

A single 17-kDa band was detected for superoxide dismutase (SOD) (Fig. 5). Drought decreased SOD accumulation in the ds group at t1 (Fig. 6D). The values were similar in the ww and ds groups during recovery. At t3, the strongest signal was observed in the ww-ww condition. All other conditions showed lower values, with particularly significant reductions in the ww-ds, ds-ww, and ds-ds conditions.

A Western blot analysis using an HSP70 antibody was conducted (Fig. 5). As can be seen in Fig. 6E, during the early-short stress at t1 HSP70 levels were higher under ds condition than under ww condition. Conversely, during recovery at t2, HSP70 levels were lower under ds condition than under ww conditions.

Western blotting revealed a 5-enolpyruvylshikimate-3-phosphate synthase (EPSPS) band at 48 kDa (Fig. 5). Quantification of EPSPS (Fig. 6F) shows an accumulation of this enzyme in the ds group compared to the control at both t1 and t2. Under late-long drought at t3, the highest level of EPSPS accumulation was recorded in the ds-ww group. In the other groups the accumulation of EPSPS was lower.

An 81 kDa band was observed for phenylalanine ammonia-lyase (PAL) (Fig. 5). During the early-short drought stress, PAL accumulated more in ds than in ww (see Fig. 6G). The PAL content in ww and ds was identical during recovery. At t3, the highest PAL content was found in the ds-ww group. Of the stressed groups, the ww-ds group had half the PAL content of the ds-ds group. Similar to the trend observed for other proteins (e.g. HSP70 and EPSPS), PAL levels were highest in the ds-ww group at t3 and lower in all the other conditions.

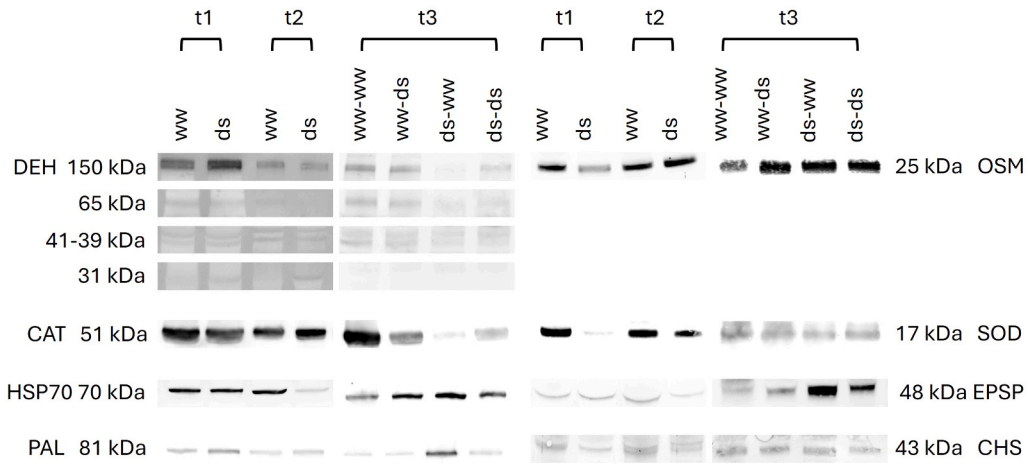


Fig. 5. Western blot analysis of stress-responsive proteins. Total protein extracts analyzed at different time points (t1, t2, t3) under well-watered (ww), drought-stress (ds) and their combination conditions. For two-letter treatment codes, the first 'ds' acronym indicates the early-short stage of water deficit and the second 'ds' indicates the late-long stage of drought. Molecular weights (kDa) and corresponding proteins are indicated: dehydrin (DEH, 150, 65, 41, 39 and 31 kDa), catalase (CAT, 51 kDa), heat shock protein 70 (HSP70, 70 kDa), phenylalanine ammonia-lyase (PAL, 81 kDa), osmotin (OSM, 25 kDa), superoxide dismutase (SOD, 17 kDa), 5-enolpyruvylshikimate-3-phosphate synthase (EPSP, 48 kDa), and chalcone synthase (CHS, 43 kDa).

Lastly, western blotting using an anti-chalcone synthase (CHS) antibody revealed an immunoreactive band at 43 kDa (Fig. 5). Fig. 6H shows that at t1, the levels of CHS was low, with the ds group showing higher accumulation than the ww group at both t1 and t2. At t3, the CHS level was highest in the ww-ww group, while accumulation was lower and similar in all the other groups that had been subjected to one or both drought stress periods.

4. Discussion

4.1. Water management regulation and stomatal control

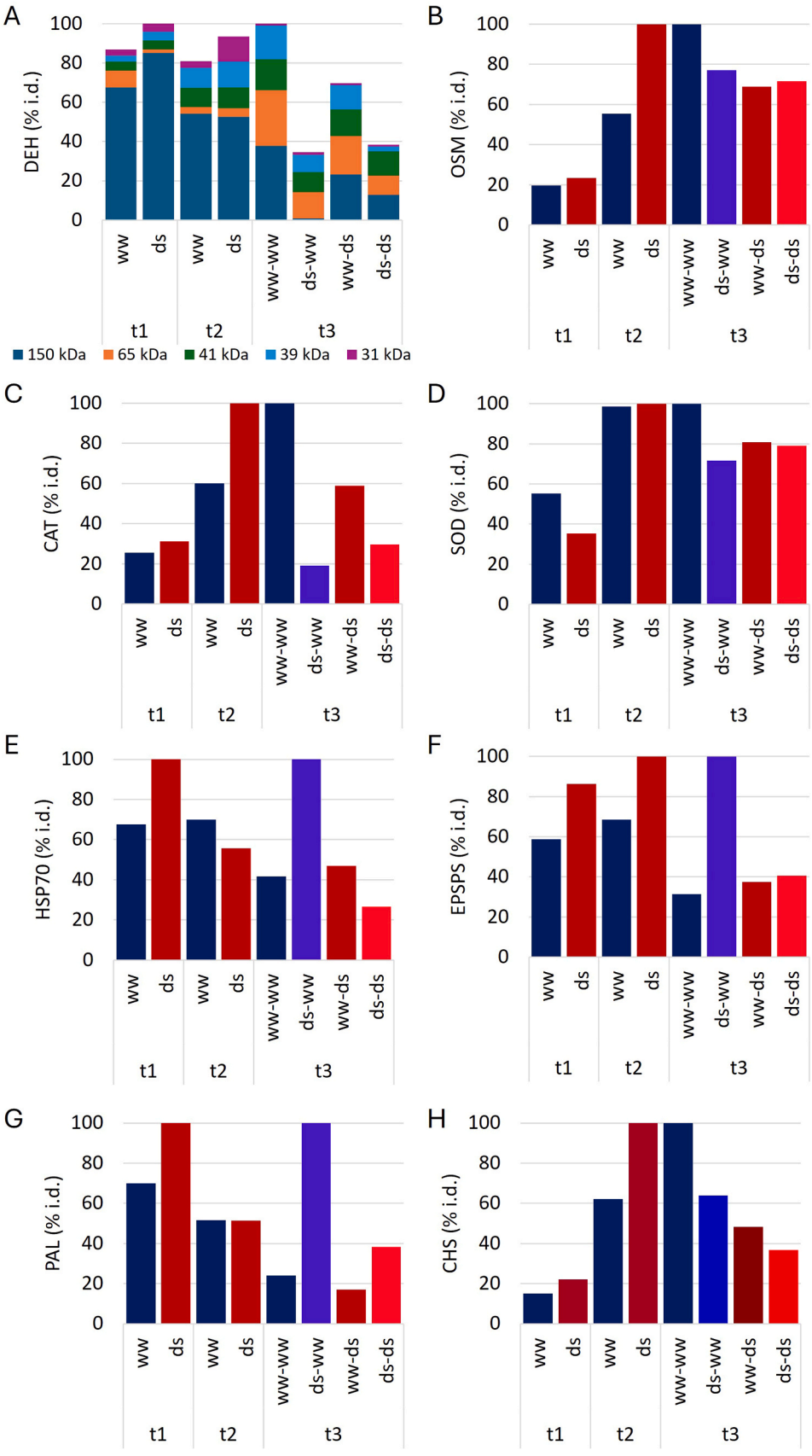
Our results show that the water management and metabolic strategies of the M2 rootstock diverge under recurrent drought. Although prior exposure to water deficit does not provide a competitive advantage in terms of stomatal regulation or the maintenance of water status, the patterns of protein accumulation are consistent with a potential biochemical imprint that preserves cellular integrity during subsequent stress events. Specifically, stomatal conductance decreased rapidly and markedly in all drought-stressed groups during both stress periods, with no significant difference between ds-ds and ww-ds at t3, indicating that prior exposure to drought conferred no physiological advantage on stomatal control. Net carbon assimilation followed the same pattern as g_{sw}, declining in all stressed groups as a direct consequence of stomatal closure, which limits CO_2 entry into the mesophyll (Chaves et al., 2010; Lovisolo et al., 2010). Similarly, no difference due to the prior exposition to the stress were found in RWC. However, despite statistically significant differences in RWC between stressed and well-watered groups, the absolute values remained relatively high (approximately 85–87%) in all stressed groups. These results suggest that M2 prioritises water conservation through early stomatal closure at the cost of reduced photosynthetic activity and increased susceptibility to oxidative stress (Anichini et al., 2026a; Pereira et al., 2026). A comparable coupling between early stomatal limitation, the maintenance of relative water content and the associated photo-oxidative load has been reported in grapevine saplings subjected to progressive water deficit (Daler et al., 2024b).

The absence of a priming advantage at a level of water management is further supported by water-related protein accumulation patterns: dehydrins, which accumulated in drought-stressed plants at t1, and osmotin, which reached its maximum accumulation during recovery at t2, were not further induced in the stressed groups at t3. This suggests that the plant does not reinvest in these osmo-protective proteins during the late-long stress event. A similar temporal pattern has been reported for HSP70, which plays a key role in preventing protein denaturation during osmotic stress (Anichini et al., 2026b; Liu et al., 2022). Taken together, these results suggest that once stomata close and water conservation begins, M2 plants redirect their adaptive investment away from costly osmotic adjustment proteins, prioritising water retention over increased oxidative risk. Therefore, the effects of oxidative stress and the antioxidant response are crucial factors to consider when evaluating the impact of stress memory.

4.2. Membrane integrity and non-enzymatic antioxidant priming

Indeed, the most compelling evidence for a functional advantage conferred by prior drought exposure came from electrolyte leakage measurements. This is a measure of membrane integrity that is closely linked to the capacity to scavenge ROS, which accumulate in chloroplasts under drought during stomatal closure and cause lipid peroxidation and membrane disruption (Peng et al., 2023). At t3, the ww-ds group exhibited significantly higher EL, indicating greater membrane damage than the ds-ds group whose membrane permeability values were statistically equivalent to those of the ww-ww and ds-ww controls;. Nevertheless, the photosynthetic machinery did not show permanent damage in any of the experimental groups, as demonstrated by F_v/F_m measurements. However, its actual photosynthetic performance was affected by water deficit during both stress periods, with the same effect observed across all ds groups. This pattern suggests that the protection observed in ds-ds is the result of a potential priming-induced protective mechanism at the membrane level. Based on protein abundance, the protective advantage observed in ds-ds compared to ww-ds appears to be primarily non-enzymatic in nature rather than due to the upregulation of the classical ROS-scavenging enzymatic system, as SOD and CAT did not show higher accumulation in ds-ds than in ww-ds. This is demonstrated by the significant increase in total polyphenol and flavonoid content in ds-ds at t3. This interpretation is consistent with studies in which improved membrane stability under water deficit was associated with a higher phenolic and flavonoid pool rather than with a proportional rise in SOD or CAT abundance, supporting the view that the non-enzymatic fraction can be the primary determinant of membrane protection in grapevine (Daler and Kaya, 2024; Daler et al., 2025).

Drought-induced enrichment of the phenylpropanoid and flavonoid biosynthesis pathways has been confirmed at the transcriptomic and metabolomic levels in grapevine (Chambard et al., 2026), and CHS



(caption on next page)

Fig. 6. Densitometric quantification of stress-responsive proteins. Relative abundance (% integrated density, i.d.) of (A) dehydrin (DEH), (B) osmotin (OSM), (C) catalase (CAT), (D) superoxide dismutase (SOD), (E) heat shock protein 70 (HSP70), (F) 5-enolpyruvylshikimate-3-phosphate synthase (EPSPS), (G) phenylalanine ammonia-lyase (PAL), and (H) chalcone synthase (CHS), measured at time points t1, t2, and t3. Bars represent the following treatments: ww (well-watered), ds (drought-stressed), and their combinations across experimental phases (ww-ww, ww-ds, ds-ww, ds-ds). In (A) and (H), coloured segments indicate distinct molecular weight isoforms (kDa) as specified in the respective legends. Within each panel, data are normalised to the highest band intensity, separately for the t1–t2 and t3 datasets (100% = maximum signal within each normalisation set).

protein accumulation has been shown to correlate positively with total flavonoid content across grapevine organs under drought stress (Wang et al., 2016). Conversely, a reduction in CHS expression under water deficit conditions may indicate that the 4-coumaroyl-CoA pool, the common substrate downstream of PAL, is being diverted from the flavonoid biosynthesis pathway towards stilbene synthase (STS). This favours the production of resveratrol, which is one of the grapevine's main bioactive compounds involved in defence against abiotic stress (Sun et al., 2023). In this study, the polyphenol and flavonoid levels were comparable to the ww-ww during early-short stress (t1) and recovery phase (t2). This rules out the possibility that the higher antioxidant pool observed in ds-ds at t3 is simply due to the retention of metabolites synthesised during the first stress. EPSPS, PAL and CHS, the key enzymes of the shikimate and phenylpropanoid pathways (Fig. 7), respectively, were accumulated in drought-stressed plants at t1 and during recovery at t2. This may suggest a different mechanism: the first stress event may have resulted in a biochemical imprint, possibly reflected in an accumulation of specific enzymes of the polyphenol and flavonoid biosynthetic pathway which could enable a faster response when the second stress event occurs.

This interpretation is supported by literature on stress memory in other species. In wheat, PAL has been identified as a memory re-triggering gene, showing markedly higher expression in primed plants upon a subsequent stress compared to non-primed controls (Wang et al., 2025). Similarly, seed-priming experiments in wheat revealed that activation of the phenylpropanoid biosynthesis pathway is a key component of stress memory, enabling the rapid production of defensive secondary metabolites upon re-stress (Decsi et al., 2025). In grapevine specifically, EPSPS and PAL expressions have been shown to increase in response to declining water potential, with concomitant activation of downstream metabolite synthesis (Strah et al., 2026). The role of chromatin modifications in maintaining this biosynthetic priming between stress events is also worth noting: epigenetic bookmarks associated with flavonoid biosynthesis genes have been identified as potential mechanisms for retaining metabolic memory across recovery periods (Bulgakov, 2024).

The accumulation of EPSPS and PAL in ds-ww plants at t3, while polyphenol and flavonoid content remained low and comparable to that of the control, suggests the existence of potential enzymatic memory and a state of metabolic alertness. The upstream biosynthetic machinery is maintained in an active configuration, poised to produce secondary metabolites rapidly if a second stress is imposed, but the costly accumulation of end-products is suppressed in the absence of a triggering stress. This is consistent with the resource-saving model of priming, in which plants retain enzymatic readiness without investing in full-scale secondary metabolite synthesis unless the triggering stress occurs (Bruce et al., 2007; Hilker and Schmülling, 2019). Importantly, the persistence of EPSPS and CHS during recovery (ds-ww), without the immediate accumulation of polyphenols, suggests that high protein abundance represents a state of 'priming readiness', rather than active metabolic flow. When exposed to a second stress (ds-ds), this pre-formed enzymatic machinery could be rapidly activated, enabling a quick accumulation of protective secondary metabolites and bypassing the lag phase of de novo protein synthesis. Once the antioxidant pool is sufficient for cellular defence, the degradation of these biosynthetic enzymes could be enhanced to save amino acids and conserve resources. Future studies including enzymatic activity assays would help to confirm this hypothesis.

4.3. *The supporting role of soluble sugars*

Finally, glucose and fructose accumulated significantly in the ds-ds group at t3, while remaining comparable to the ww-ww control in all other groups regardless of their current irrigation status. Given that there is no advantage in water status management, their role is unlikely to be primarily osmotic. One possible interpretation is that glucose and fructose may contribute to the non-enzymatic antioxidant response by acting as ROS scavengers and membrane stabilisers under drought conditions, as suggested by Krishankumar et al. (2025). They stated that the accumulation of these sugars has been associated with improved membrane integrity and ROS detoxification capacity in grafted grapevines. Sugars, particularly sucrose, may also play a role in inducing PAL activity (Ferrandino et al., 2023; Pirie and Mullins, 1976). However, the potential role of these sugars in scavenging ROS has yet to be tested

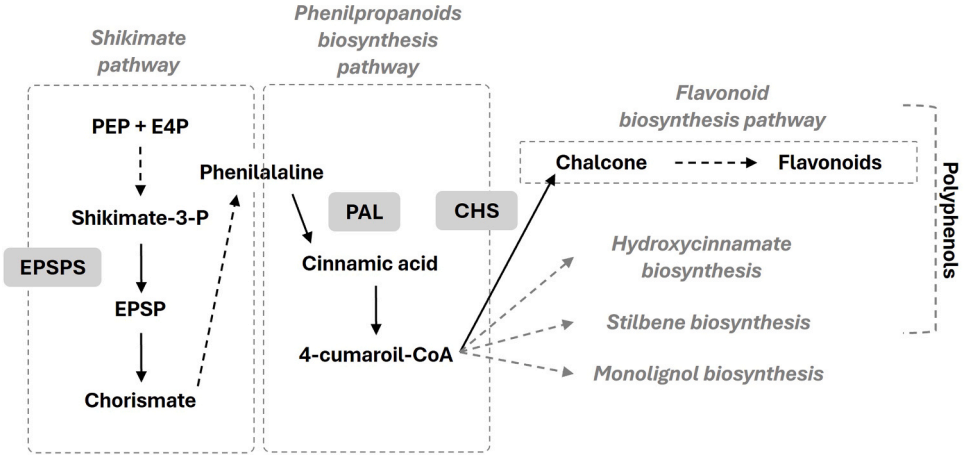


Fig. 7. Overview of the biosynthetic pathways investigated in this study. The shikimate pathway, phenylpropanoid biosynthesis pathway, and downstream branches are shown, with the enzymes quantified in this study (EPSPS, PAL and CHS) highlighted in grey boxes. Solid arrows indicate direct enzymatic reactions; dashed arrows indicate multi-step routes leading to the major polyphenolic end-products. The colour grey indicates that the parameters were not measured in this study.

directly in further studies.

5. Conclusion

While stress memory in grapevines has been studied in the context of structural and epigenetic adaptations to recurrent drought across growing seasons, the biochemical mechanisms underlying short-term, within-season stress memory remain poorly understood. The present findings suggest that repeated brief drought events leave a biochemical imprint on the non-enzymatic antioxidant biosynthetic pathway. This primes the pathway's enzymatic machinery to respond faster and more robustly to re-stress.

Returning to the three hypotheses formulated in the introduction, the results allow the following conclusions to be drawn.

Hypothesis (i). which states that plants exposed to repeated drought events will exhibit enhanced tolerance compared to non-primed plants, is partially supported. No advantage was observed in terms of water management, whereas tolerance to oxidative stress was enhanced.

Hypothesis (ii). which states that the primed state is associated with specific biochemical adjustments that persist after recovery or are reactivated more rapidly upon re-stress, is supported by the protein data. It appears that maintaining the enzymes of the shikimate and phenylpropanoid pathways during recovery laid the groundwork for increased polyphenol and flavonoid production in response to repeated drought stress.

Hypothesis (iii). which states that primed plants will display pre-accumulation or rapid re-induction of antioxidant compounds, is supported. Rather than maintaining high baseline levels of the energy-expensive end products during stress-free periods, the M2 genotype utilises a rapid re-induction model. When faced with a second stress, plants activate flavonoid and polyphenol biosynthesis to a significantly greater extent than those experiencing the stress for the first time, thanks to the accumulation of the upstream enzyme.

This fine regulation must be investigated further, bearing in mind the two potential limitations of the present study. Firstly, the experiments were conducted on rooted M2 cuttings as an autonomous root-canopy system. While this approach was essential for analysing the biochemical memory of the M2 genotype without the influence of vascular interactions, further studies are required to determine whether this memory imprint is transferred through the graft union in scion-rootstock combinations. Secondly, although growth chamber studies provide the highly controlled environment necessary to isolate priming mechanisms, field validation under multiple stress conditions is crucial to confirm the agronomic relevance of short-term drought priming in viticulture.

CRediT authorship contribution statement

Sara Parri: Writing – original draft, Methodology, Data curation, Conceptualization. **Sara Anichini:** Writing – original draft, Methodology, Data curation, Conceptualization. **Marco Romi:** Validation, Resources, Funding acquisition. **Luigi Falginella:** Writing – review & editing, Resources. **Elisa De Luca:** Writing – review & editing, Resources. **Giampiero Cai:** Writing – original draft, Supervision, Conceptualization.

Declaration of Competing Interest

The authors declare that they have no known competing financial interests or personal relationships that could have appeared to influence the work reported in this paper.

Acknowledgements

The authors would like to express their gratitude to the Santa Chiara Lab at the University of Siena, Italy (https://santachiaralab.unisi.it/), particularly to Prof. Angelo Riccaboni and Dr. Cristiana Tozzi, for granting us access to the Microcosmo equipment in the Farming Lab. This equipment was acquired through the Metrofood Italia project (www.metrofood.it). We thank the Tuscany Region for supporting the Ph.D. grant of Sara Anichini in the framework of 'Pegaso' - POR FSE TOSCANA 2014–2020 Program GiovaniSì. We would also like to thank Prof. Silvia Casini and her team in the Department of Physical, Environmental and Earth Sciences at the University of Siena for the access to the microplate reader used for the colorimetric assays. We would also like to thank Sara Monaci for kindly performing the gas exchange measurements as part of her thesis work.

References

Anichini, S., Cai, G., Betti, T., Romi, M., Bianchi, D., Brancadoro, L., Parri, S., 2026a. Integrated physiological and biochemical screening of commercial and novel grapevine rootstocks under drought stress. Sci. Hortic. 365, 114984. https://doi.org/10.1016/j.scienta.2026.114984.

Anichini, S., Parri, S., Bellini, A., Faleri, C., Romi, M., Falginella, L., Cai, G., 2026b. Distinct root signaling and anatomy associate with convergent leaf responses to drought and salinity in grapevine rootstocks. Plant Physiol. Biochem. PPB 238, 111680. https://doi.org/10.1016/j.plaphy.2026.111680.

Botton, A., Girardi, F., Ruperti, B., Brilli, M., Tijero, V., Eccher, G., Populin, F., Schievano, E., Riello, T., Munné-Bosch, S., Canton, M., Rasori, A., Cardillo, V., Meggio, F., 2022. Grape berry responses to sequential flooding and heatwave events: a physiological, transcriptional, and metabolic overview. Plants 11. https://doi.org/10.3390/plants11243574.

Bruce, T.J.A., Matthes, M.C., Napier, J.A., Pickett, J.A., 2007. Stressful "memories" of plants: Evidence and possible mechanisms. Plant. Sci. 173, 603–608. https://doi.org/10.1016/j.plantsci.2007.09.002.

Bulgakov, V.P., 2024. Chromatin modifications and memory in regulation of stress-related polyphenols: finding new ways to control flavonoid biosynthesis. Crit. Rev. Biotechnol. 44, 1478–1494. https://doi.org/10.1080/07388551.2024.2336529.

Canton, M., Mirone, F., Meggio, F., Pichierri, A., Casolo, V., Tornielli, G.B., Pitacco, A., 2025. Consecutive moderate and severe drought stresses affect chlorophyll fluorescence and non-structural carbohydrates dynamics in grapevine leaves. Physiol. Plant. 177, e70535. https://doi.org/10.1111/ppl.70535.

Chambard, M., Cantù, D., Bortolami, G., Dell'Acqua, N., Ferrer, N., Gambetta, G.A., Garcia, J.F., Gastou, P., Massonnet, M., Moretti, S., Rochepeau, A., Pétriacq, P., Foulongne-Oriol, M., Delmas, C.E.L., 2026. Fungal pathogen activity and stress-dependent responses of grapevine wood to esca and drought. Physiol. Plant. 178, e70914. https://doi.org/10.1111/ppl.70914.

Chaves, M.M., Zarrouk, O., Francisco, R., Costa, J.M., Santos, T., Regalado, A.P., Rodrigues, M.L., Lopes, C.M., 2010. Grapevine under deficit irrigation: hints from physiological and molecular data. Ann. Bot. 105, 661–676. https://doi.org/10.1093/aob/mcq030.

Daler, S., Kaya, O., 2024. Exogenous alpha-lipoic acid treatments reduce the oxidative damage caused by drought stress in two grapevine rootstocks. Physiol. Plant. 176, e14437. https://doi.org/10.1111/ppl.14437.

Daler, S., Kaya, O., Canturk, S., Korkmaz, N., Kılıç, T., Karadağ, A., Hatterman-Valenti, H., 2025. Silicon nanoparticles (SiO_2 NPs) boost drought tolerance in grapevines by enhancing some morphological, physiological, and biochemical traits. Plant. Mol. Biol. Rep. 43, 1057–1075. https://doi.org/10.1111/ppl.14437.

Daler, S., Kaya, O., Korkmaz, N., Kılıç, T., Karadağ, A., Hatterman-Valenti, H., 2024b. Titanium nanoparticles (TiO_2-NPs) as catalysts for enhancing drought tolerance in grapevine saplings. Horticulturae 10, 1103. https://doi.org/10.3390/horticulturae10101103.

Daler, S., Korkmaz, N., Kılıç, T., Hatterman-Valenti, H., Karadağ, A., Kaya, O., 2024a. Modulatory effects of selenium nanoparticles against drought stress in some grapevine rootstock/scion combinations. Chem. Biol. Technol. Agric. 11, 108. https://doi.org/10.1186/s40538-024-00609-6.

Decsi, K., Ahmed, M., Abdul-Hamid, D., Rizk, R., Tóth, Z., 2025. Verification of seed-priming-induced stress memory by genome-wide transcriptomic analysis in wheat (*Triticum aestivum* L.). Agronomy 15, 1365. https://doi.org/10.3390/agronomy15061365.

Dinis, L.-T., Bernardo, S., Luzio, A., Pinto, G., Meijón, M., Pintó-Marijuan, M., Cotado, A., Correia, C., Moutinho-Pereira, J., 2018. Kaolin modulates ABA and IAA dynamics and physiology of grapevine under Mediterranean summer stress. J. Plant. Physiol. 220, 181–192. https://doi.org/10.1016/j.jplph.2017.11.007.

El Yamani, M., Sakar, E.H., Boussakouran, A., Rharrabti, Y., 2019. Physiological and biochemical responses of young olive trees (*Olea europaea* L.) to water stress during flowering. Arch. Biol. Sci. 71, 123–132. https://doi.org/10.2298/ABS181001054E.

Ferrandino, A., Pagliarani, C., Pérez-Álvarez, E.P., 2023. Secondary metabolites in grapevine: crosstalk of transcriptional, metabolic and hormonal signals controlling stress defence responses in berries and vegetative organs. Front. Plant. Sci. 14. https://doi.org/10.3389/fpls.2023.1124298.

Hajizadeh Sisakhti, S., Dehdari, M., Ebrahimi, M.A., 2025. Responses of some important physiological traits of regenerated plantlet grape (*Vitis vinifera* L.) genotypes to cold stress. Discov. Plants 2 (1), 120. https://doi.org/10.1007/s44372-025-00202-7.

Hilker, M., Schmülling, T., 2019. Stress priming, memory, and signalling in plants. Plant. Cell. Environ. 42, 753–761. https://doi.org/10.1111/pce.13526.

Kar, S., Montague, T., Villanueva-Morales, A., Hellman, E., 2021. Measurement of gas exchange on excised grapevine leaves does not differ from in situ leaves, and potentially shortens sampling time. Appl. Sci. 11 (8), 3644.

Krishankumar, S., Hunter, J.J., Alyafei, M., Souka, U., Subramaniam, S., Ramlal, A., Kurup, S.S., Amiri, K.M.A., 2025. Influence of different scion-rootstock combinations on sugars, polyamines, antioxidants and malondialdehyde in grafted grapevines under arid conditions. Front. Plant. Sci. 16, 1559095. https://doi.org/10.3389/fpls.2025.1559095.

Król, A., Weidner, S., 2017. Changes in the proteome of grapevine leaves (*Vitis vinifera* L.) during long-term drought stress. J. Plant. Physiol. 211, 114–126. https://doi.org/10.1016/j.jplph.2016.11.016.

Lämke, J., Bäurle, I., 2017. Epigenetic and chromatin-based mechanisms in environmental stress adaptation and stress memory in plants. Genome Biol. 18, 124. https://doi.org/10.1186/s13059-017-1263-6.

Liu, X., Chen, H., Li, S., Wang, L., 2022. Genome-wide identification of the Hsp70 gene family in grape and their expression profile during abiotic stress. Horticulturae 8, 743. https://doi.org/10.3390/horticulturae8080743.

Lovisolo, C., Perrone, I., Carra, A., Ferrandino, A., Flexas, J., Medrano, H., Schubert, A., 2010. Drought-induced changes in development and function of grapevine (*Vitis* spp.) organs and in their hydraulic and non-hydraulic interactions at the whole-plant level: a physiological and molecular update. Funct. Plant. Biol. 37, 98–116. https://doi.org/10.1071/FP09191.

Merli, M.C., Magnanini, E., Gatti, M., Pirez, F.J., Pueyo, I.B., Intrigliolo, D.S., Poni, S., 2016. Water stress improves whole-canopy water use efficiency and berry composition of cv. Sangiovese (*Vitis vinifera* L.) grapevines grafted on the new drought-tolerant rootstock M4. Agric. Water Manag. 169, 106–114. https://doi.org/10.1016/j.agwat.2016.02.025.

Munitz, S., Netzer, Y., Shtein, I., Schwartz, A., 2018. Water availability dynamics have long-term effects on mature stem structure in *Vitis vinifera*. Am. J. Bot. 105, 1443–1452. https://doi.org/10.1002/ajb2.1148.

Nagahatenna, D.S.K., Furlan, T.S., Edwards, E.J., Ramesh, S.A., Pagay, V., 2022. Insights into long-term acclimation strategies of grapevines (*Vitis vinifera* L.) in response to multi-decadal cyclical drought. Agronomy 12, 3221. https://doi.org/10.3390/agronomy12123221.

Netzer, Y., Munitz, S., Shtein, I., Schwartz, A., 2019. Structural memory in grapevines: Early season water availability affects late season drought stress severity. Eur. J. Agron. 105, 96–103. https://doi.org/10.1016/j.eja.2019.02.008.

Parri, S., Faleri, C., Romi, M., Del Río, J.C., Rencoret, J., Dias, M.C.P., Anichini, S., Cantini, C., Cai, G., 2024. Unravelling different water management strategies in three olive cultivars: the role of osmoprotectants, proteins, and wood properties. Int. J. Mol. Sci. 25, 11059. https://doi.org/10.3390/ijms252011059.

Parri, S., Romi, M., Hoshika, Y., Giovannelli, A., Dias, M.C., Piritore, F.C., Cai, G., Cantini, C., 2023. Morpho-physiological responses of three Italian olive tree (*Olea europaea* L.) cultivars to drought stress. Horticulturae 9, 830. https://doi.org/10.3390/horticulturae9070830.

Peng, Y., Chen, J., Long, W., He, P., Zhou, Q., Hu, X., Zhou, Y., Zheng, Y., 2023. Transcriptomic and metabolomic analyses of seedlings of two grape cultivars with distinct tolerance responses to flooding and post-flooding stress conditions. Horticulturae 9, 980. https://doi.org/10.3390/horticulturae9090980.

Pereira, J.P., Bevilacqua, I., Santos, R.B., Varotto, S., Chitarra, W., Nerva, L., Figueiredo, A., 2025. Epigenetic regulation and beyond in grapevine-pathogen interactions: a biotechnological perspective. Physiol. Plant. 177, e70216. https://doi.org/10.1111/ppl.70216.

Pereira, Sara, Moutinho-Pereira, J.M., Maia, C., Moura, R., Brito, C., Dinis, L.-T., Pereira, Sandra, 2026. Impact of cultivar on grapevine physiological adaptation to drought and subsequent rehydration. Front. Plant. Sci. 17. https://doi.org/10.3389/fpls.2026.1757730.

Pirie, A., Mullins, M.G., 1976. Changes in anthocyanin and phenolics content of grapevine leaf and fruit tissues treated with sucrose, nitrate, and abscisic acid. Plant. Physiol. 58, 468–472. https://doi.org/10.1104/pp.58.4.468.

Sadhukhan, A., Prasad, S.S., Mitra, J., Siddiqui, N., Sahoo, L., Kobayashi, Y., Koyama, H., 2022. How do plants remember drought? Planta 256, 7. https://doi.org/10.1007/s00425-022-03924-0.

Singleton, V.L., Rossi, J.A., 1965. Colorimetry of total phenolics with phosphomolybdic-phosphotungstic acid reagents. Am. J. Enol. Vitic. 16, 144–158. https://doi.org/10.5344/ajev.1965.16.3.144.

Smirnova, L.P., Pervykh, L.N., 1998. Quantitative determination of the total content of flavonoids in the flowers of immortelle *Helichrysum arenarium*. Pharm. Chem. J. 32, 321–324. https://doi.org/10.1007/BF02580519.

Strah, R., Falchi, R., Song, C., Blejec, A., Ramšak, I., Gruden, K., Peterlunger, E., Fait, A., Pompe Novak, M., Sivilotti, P., 2026. Combined omics data reveal multilevel response to water deficit in grapevine disease- resistant varieties. Front. Plant. Sci. 17, 1818883. https://doi.org/10.3389/fpls.2026.1818883.

Sun, H.-T., Zuo, D.-D., Pei, M.-S., Liu, H.-N., Wei, T.-L., Guo, D.-L., 2024. Transcriptome analysis revealed the stress memory of grapes after hydrogen peroxide acclimation treatment. Sci. Hortic. 328, 112938. https://doi.org/10.1016/j.scienta.2024.112938.

Sun, Y., Xi, B., Dai, H., 2023. Effects of water stress on resveratrol accumulation and synthesis in 'Cabernet Sauvignon' grape berries. Agronomy 13. https://doi.org/10.3390/agronomy13030633.

Tombesi, S., Frioni, T., Poni, S., Palliotti, A., 2018. Effect of water stress "memory" on plant behavior during subsequent drought stress. Environ. Exp. Bot. 150, 106–114. https://doi.org/10.1016/j.envexpbot.2018.03.009.

Venios, X., Gkizi, D., Nisiotou, A., Korkas, E., Tjamos, S.E., Zamioudis, C., Banilas, G., 2024. Emerging roles of epigenetics in grapevine and winegrowing. Plants 13. https://doi.org/10.3390/plants13040515.

Villalobos-Soublett, E., Verdugo-Vásquez, N., Díaz, I., Zurita-Silva, A., 2022. Adapting grapevine productivity and fitness to water deficit by means of naturalized rootstocks. Front. Plant. Sci. 13, 870438.

Wang, H., Wang, W., Zhan, J., Yan, A., Sun, L., Zhang, G., Wang, X., Ren, J., Huang, W., Xu, H., 2016. The accumulation and localization of chalcone synthase in grapevine (*Vitis vinifera* L.). Plant. Physiol. Biochem. 106, 165–176. https://doi.org/10.1016/j.plaphy.2016.04.042.

Wang, Y., Zheng, L., Song, J., Cai, J., Zhou, Q., Zhong, Y., Jiang, D., Wang, X., 2025. Drought priming-induced low temperature stress tolerance in wheat: insight into stress memory dynamics. Crop. Environ. 4, 118–129. https://doi.org/10.1016/j.crope.2025.03.003.

Winkel-Shirley, B., 2002. Biosynthesis of flavonoids and effects of stress. Curr. Opin. Plant. Biol. 5, 218–223. https://doi.org/10.1016/S1369-5266(02)00256-X.

Zamorano, D., Franck, N., Pastenes, C., Wallberg, B., Garrido, M., Silva, H., 2021. Improved physiological performance in grapevine (*Vitis vinifera* L.) cv. Cabernet Sauvignon facing recurrent drought stress. Aust. J. Grape Wine Res. 27, 258–268. https://doi.org/10.1111/ajgw.12482.

Zhu, Z., Li, Q., Gichuki, D.K., Hou, Y., Liu, Y., Zhou, H., Xu, C., Fang, L., Gong, L., Zheng, B., Duan, W., Fan, P., Wang, Q., Xin, H., 2023. Genome-wide profiling of histone H3 lysine 27 trimethylation and its modification in response to chilling stress in grapevine leaves. Hortic. Plant. J. 9, 496–508. https://doi.org/10.1016/j.hpj.2023.03.002.

Zuo, D.-D., Sun, H.-T., Yang, L., Zheng, M.-L., Zhang, J., Guo, D.-L., 2024. Hydrogen peroxide priming triggers splicing memory in grape berries. Plant. Mol. Biol. 114, 129. https://doi.org/10.1007/s11103-024-01528-8.